sarily imply an identical transition state; the rough proportionality between the number of N atoms and terrace width rather suggests that the product atoms remain largely on the side from which the NO molecule approached the step. If the highly coordinated atoms at the bottom of the steps were active, as proposed in (6), the presence of the N atoms at the upper sides could not be accounted for. That the N atoms themselves move across the steps is ruled out by the finding that the numbers of N atoms on each side remained constant over at least 2 hours after NO adsorption. During this time only diffusion away from the step was observed (*12*). Interestingly, the result that the active sites are formed by low-coordinated atoms is in agreement with the original idea of Taylor (*1*).

We propose that the active-site effect during NO dissociation is caused by changes in the *d*-band local density of states (LDOS) at the Fermi energy E_F at the steps. Electronic structure calculations have shown that the chemical behavior of transition-metal surfaces is determined mostly by the *d* states (*19*, *20*); other theoretical studies suggested that the reactivity is connected with the E_F-LDOS (*21*–*23*). For the low-coordinated atoms at the top of steps the local *d* band narrows compared to the terraces (*21*). In Ru, which is close to the center of the transition-metal row of the periodic table where E_F intersects near the center of the *d* band, this leads to a larger density of *d* states at E_F (*24*). In the case of NO dissociation, the local reactivity is most likely governed by the extent of the backbonding between *d* orbitals and the antibonding NO π^* orbital, by analogy with CO (*25*). A larger *d*-LDOS should cause a more pronounced degree of backbonding, thus weakening the N–O bond and leading to an easier bond-breaking. This is similar to the effect of coadsorbed alkali atoms (*22*) for which a "softening" of the N–O bond has been observed (*26*). Electronegative coadsorbates such as O lead to a lowering of the E_F-LDOS and hence a reverse effect (*22*) that is reflected in a "stiffening" of the N–O bond (*9*). The deactivation of the type I steps by trapped O atoms is fully consistent with this picture.

These data directly confirm the concept of active sites in heterogeneous catalysis but demonstrate that the kinetics expressed as a "turnover frequency" (*2*, *3*) will be influenced by the microscopic surface structure and composition in a rather complex manner. For "real" catalysis under steady-state flow conditions, less active sites (for example, on terraces) will certainly come into play, so that the overall reactivity will be the result of weighted contributions from various surface structure elements, dominated by the active sites. This is, for example, reflected in the appreciably faster rate of hydrogenation of NO at 450 K on a stepped rather than on a flat Ru(0001) surface (*27*).

REFERENCES AND NOTES

1. H. S. Taylor, *Proc. R. Soc. London Ser. A* **108**, 105 (1925).
2. M. Boudart, *Adv. Catal.* **20**, 153 (1969).
3. ——— and G. Djéga-Mariadassou, *Kinetics of Heterogeneous Catalytic Reactions* (Princeton Univ. Press, Princeton, NJ, 1984).
4. G. M. Schwab and E. Pietsch, *Z. Phys. Chem. Abt. B* **1**, 385 (1929).
5. See, for example, G. A. Somorjai, R. W. Joyner, B. Lang, *Proc. R. Soc. London Ser. A* **331**, 335 (1972).
6. L. M. Falicov and G. A. Somorjai, *Proc. Natl. Acad. Sci. U.S.A.* **82**, 2207 (1985).
7. T. P. Kobylinski and B. W. Taylor, *J. Catal.* **33**, 376 (1974).
8. E. Umbach, S. Kulkarni, P. Feulner, D. Menzel, *Surf. Sci.* **88**, 65 (1979).
9. H. Conrad, R. Scala, W. Stenzel, R. Unwin, *ibid.* **145**, 1 (1984).
10. J. Trost, T. Zambelli, J. Wintterlin, G. Ertl, in preparation.
11. That both are imaged dark, that is, as depressions, is an electronic effect that is well understood for O [N. D. Lang, *Commun. Condens. Matter Phys.* **14**, 253 (1989)]. The imaging difference between N and O may be caused by different electronegativities or the different energies of the N and O 2*p* states.
12. T. Zambelli, J. Trost, J. Wintterlin, G. Ertl, *Phys. Rev. Lett.* **76**, 795 (1996).
13. Earlier measurements (*12*) have shown that the mobility of the N atoms is not significantly affected by the STM tip.
14. M. Lindroos, H. Pfnür, G. Held, D. Menzel, *Surf. Sci.* **222**, 451 (1989).
15. P. Feulner, S. Kulkarni, E. Umbach, D. Menzel, *ibid.* **99**, 489 (1980).
16. G. E. Thomas and W. H. Weinberg, *Phys. Rev. Lett.* **41**, 1181 (1978).
17. With $\tau_{des} = \tau_0 \exp(E^*_{des}/kT)$ and using a desorption energy E^*_{des} of about 1.5 eV (*15*) and 10^{-13} s for τ_0, the mean residence time τ_{des} of an NO molecule on the surface is nominally 10^{12} s at 300 K. If we assume a diffusion barrier of 1/5 of E^*_{des}, which is typical for adsorbates, a mean residence time on a specific adsorption site of 10^{-8} s can be estimated analogously. With an activation energy for dissociation of about 0.7 eV [P. A. Thiel, W. H. Weinberg, J. T. Yates, *Chem. Phys. Lett.* **67**, 403 (1979)], the lifetime for a molecule at a step is of the order of 10^{-2} s before the molecule dissociates.
18. D. F. Johnson and W. H. Weinberg, *J. Chem. Phys.* **101**, 6289 (1994).
19. R. Hoffmann, *Rev. Mod. Phys.* **60**, 601 (1988).
20. B. Hammer and J. K. Nørskov, *Surf. Sci.* **343**, 211 (1995).
21. J. Tersoff and L. M. Falicov, *Phys. Rev. B* **24**, 754 (1981).
22. P. Feibelman and D. R. Hamann, *Surf. Sci.* **149**, 48 (1985).
23. This is a simplified picture, and a more recent study (*20*) pointed out that the entire valence band may play a role.
24. Tersoff and Falicov (*21*) treated Ni and Cu, which have almost filled *d* bands. For these cases a narrowing leads, in contrast to Ru, to a reduced state density at E_F, and consequently a lower reactivity of the frontmost step atom is predicted.
25. H. P. Bonzel, *Surf. Sci. Rep.* **8**, 43 (1987).
26. H. Shi, H. Dietrich, P. Geng, K. Jacobi, in preparation.
27. T. Nishida, C. Egawa, S. Naito, K. Tamaru, *J. Chem. Soc. Faraday Trans. 1* **80**, 1567 (1984).

28. We acknowledge valuable discussions with M. Scheffler and C. Stampfl, and we thank K. Jacobi for providing unpublished data. The work of T.Z. was supported by the Deutscher Akademischer Austauschdienst.

21 May 1996; accepted 2 August 1996

Self-Assembly of a Two-Dimensional Superlattice of Molecularly Linked Metal Clusters

Ronald P. Andres,* Jeffery D. Bielefeld, Jason I. Henderson, David B. Janes, Venkat R. Kolagunta, Clifford P. Kubiak, William J. Mahoney, Richard G. Osifchin

Close-packed planar arrays of nanometer-diameter metal clusters that are covalently linked to each other by rigid, double-ended organic molecules have been self-assembled. Gold nanocrystals, each encapsulated by a monolayer of alkyl thiol molecules, were cast from a colloidal solution onto a flat substrate to form a close-packed cluster monolayer. Organic interconnects (aryl dithiols or aryl di-isonitriles) displaced the alkyl thiol molecules and covalently linked adjacent clusters in the monolayer to form a two-dimensional superlattice of metal quantum dots coupled by uniform tunnel junctions. Electrical conductance through such a superlattice of 3.7-nanometer-diameter gold clusters, deposited on a SiO_2 substrate in the gap between two gold contacts and linked by an aryl di-isonitrile [1,4-di(4-isocyanophenylethynyl)-2-ethylbenzene], exhibited nonlinear Coulomb charging behavior.

A structure of great interest for developing nanoscale electronics is a planar array of small metal islands separated from each other by tunnel barriers. Electronic conduction in such a structure can be varied from the metallic to the insulating limit by controlling the size of the islands and the strength of the coupling between them. Correlated single-electron tunneling (SET) in a patterned superlattice of this type has been proposed as a future basis for nanoelectronic digital circuits (*1*). However, if

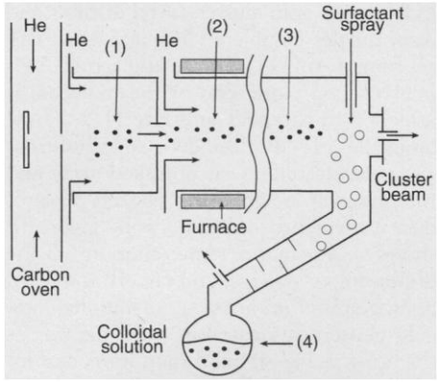

Fig. 1. Schematic of process for synthesizing a stable colloidal suspension of crystalline gold clusters. Gold atoms evaporated from a carbon crucible in a resistively heated carbon tube are entrained in He and induced to condense into nanoclusters by mixing the hot flow from the oven with a room temperature stream of He. Controlling conditions in the oven and the flow downstream from the oven (see 1) controls the mean cluster size. The clusters are melted (see 2) and recrystallized (see 3) while still in the gas phase. They are scrubbed from the gas phase by contact with a mist of organic solvent containing 1-dodecanethiol and collected as a stable colloidal suspension (see 4). Before each run, a sample of the cluster aerosol is expanded as a cluster beam into a vacuum chamber and deposited on a TEM substrate for subsequent analysis.

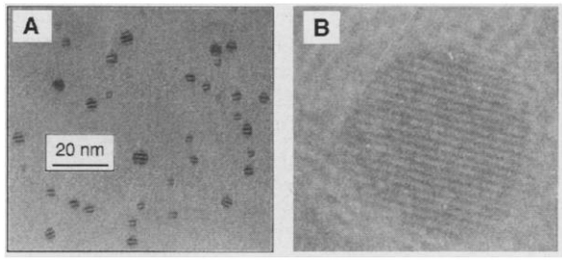

Fig. 2. Bright-field TEM micrographs of bare gold clusters. (**A**) Gold clusters supported on a thin flake of MoS_2. Each cluster exhibits moiré fringes, which indicate that the clusters are single fcc crystals. When bare gold nanocrystals are deposited on MoS_2, they spontaneously orient with a (111) facet parallel to the surface of the substrate and with the atomic rows in this facet parallel with the atomic rows in the surface plane of the substrate. (**B**) Gold cluster supported on a thin carbon film. The cluster is aligned with respect to the electron beam so that the spacing between (111) planes in the cluster is observed. These lattice fringes are 0.24 nm, which is the spacing in bulk gold.

practical devices based on SET are to be feasible, they must be fabricated by using extremely small conducting "dots" embedded in a medium free of charged impurities. SET operation at room temperature requires interdot capacitances of $\sim 1 \times 10^{-19}$ F, dictating conducting dots ~1 to 2 nm in diameter. We report on a process that makes use of molecular self-assembly to fabricate a two-dimensional (2D) superlattice of uniform metal nanocrystals linked by organic interconnects.

There are four steps involved in the synthesis of a linked cluster network (LCN): (i) synthesis of ultrafine metal crystals with uniform diameters in the nanometer range; (ii) adsorption of a self-assembled monolayer (SAM) of organic surfactant on the surface of these particles to produce stable macromolecular entities that can be manipulated; (iii) formation of a close-packed monolayer film of these coated particles on a solid substrate; and (iv) displacement of the organic surfactant with a molecular interconnect that covalently bonds adjacent particles to each other without destroying the order in the monolayer film. Although the methods we describe are quite general with respect to choice of metal, surfactant, and interconnect, we have focused on gold, dodecanethiol, and various aryl dithiols and aryl di-isonitriles.

Macromolecules with a core containing a fixed number of metal atoms surrounded by a tightly bound shell of organic ligands have been synthesized and isolated. A well-known example is $Au_{55}(PPh_3)_{12}Cl_6$, synthesized by Schmid *et al.* (*2*). Schön and Simon (*3*) discuss possible electronic applications of such metal dots. Unfortunately, only a limited number of these species have been synthesized, and displacement of their ligand shell in order to cross-link them into a LCN is difficult. A more general synthesis approach is to reduce a metal salt in an aqueous solution containing a stabilizing organic surfactant. This technique for growing small particles of controlled size is well known, and several authors describe methods for preparing "monolayers" from such colloids (*4*). However, aqueous colloids are largely charge stabilized, and it is difficult to fabricate "close-packed monolayers" of charged nanoparticles. Recently, a method has been proposed for growing uncharged gold particles in solution by using alkyl thiols as surfactants (*5*). Whetten *et al.* (*6*) have shown that nanoparticles produced by this method are equivalent in quality to clusters synthesized by the two-step method described below. Although direct solution-phase synthesis of surfactant encapsulated metal particles has the advantage of simplicity, gas-phase synthesis of bare clusters followed by solution-phase encapsulation provides greater flexibility. Ultrafine particles containing practically any atomic species and having controlled composition and size can be grown in the gas phase. In addition, separation of the particle synthesis and the particle passivation steps permits thermal annealing of the particles prior to encapsulation.

Figure 1 shows a schematic of the gas-phase cluster source that was used in the present study. A detailed description of this source can be found elsewhere (*7*). Single-component metal clusters with a controlled mean diameter in the range from 1 to 20 nm and a size distribution characterized by a full-width at half-maximum of ~0.5 nm at the low end of this range and ~5 nm at the high end have been synthesized in this source at total production rates of ~100 mg per hour.

In order to assure that all of the clusters are single crystals, a dilute aerosol stream of clusters suspended in inert gas is passed through a meter long tube in which the clusters are first heated above their melting temperature and then cooled to room temperature. Treating small gold clusters in this way transforms them into single face-centered-cubic (fcc) crystals (*8*). Figure 2 shows bright-field transmission electron microscopy (TEM) micrographs of bare gold clusters sampled from the gas phase. The most stable of these clusters appear to be truncated octahedra with eight hexagonal (111) faces and six square (100) faces. The diameter of the cluster in Fig. 2B is ~5 nm. If this cluster is a perfect truncated octahedron, it contains 6266 gold atoms.

Once gold nanocrystals of the desired size are synthesized in the gas phase, the problem remains how to capture them and assemble them into an ordered monolayer on a substrate. When bare metal clusters contact each other, they spontaneously form a twinned aggregate. Therefore the aerosol containing bare metal clusters was passed through a spray chamber in which the clusters are captured by contact with a fine spray of organic solvent and surfactant. The spray droplets are subsequently removed from the gas stream and collected in a liquid receiver. The key for successful operation of this collection technique is a surfactant that rapidly adsorbs onto the surface of the clusters and prevents aggregation. A number of molecules have been found effective in this regard, including fatty acids, alkyl thiols, alkyl disulfides, alkyl nitriles, and alkyl isonitriles. The key re-

R. P. Andres, J. D. Bielefeld, W. J. Mahoney, R. G. Osifchin, School of Chemical Engineering, Purdue University, West Lafayette, IN 47907, USA.
J. I. Henderson and C. P. Kubiak, Department of Chemistry, Purdue University, West Lafayette, IN 47907, USA.
D. B. Janes and V. R. Kolagunta, School of Electrical and Computer Engineering, Purdue University, West Lafayette, IN 47907, USA.
*To whom correspondence should be addressed.

quirements seem to be an end group that is attracted to the metal of interest and a methylene chain 8 to 12 units long to provide steric repulsion. With the proper surfactant, it is possible to capture nanometer-diameter metal clusters in various organic solvents without altering the cluster-size distribution (9). Alkyl thiols are especially effective for stabilizing small gold clusters and appear to actually improve the faceting. This phenomenon is not surprising. Poirier and Pylant (*10*) have shown that, when alkyl thiols adsorb as a SAM on Au(111), the gold surface reconstructs. We have found that 1- to 5-nm-diameter gold clusters encapsulated by 1-dodecanethiol are stable in mesitylene or decane for more than 6 months. Moreover, these particles can be treated as macromolecular entities and, by means of fractional crystallization, the cluster size distribution can be narrowed (6).

Spin casting a dilute suspension of uniform diameter, alkyl-thiol–encapsulated gold clusters in mesitylene on various flat substrates (such as highly oriented pyrolytic graphite, MoS_2, or SiO_2) produces close-packed monolayer arrays with excellent long-range order. Figure 3A is a schematic representation of the self-assembly process involved in formation of these close-packed arrays and Fig. 4A is a TEM micrograph of such an unlinked array. The mean diameter of the clusters in Fig. 4A is 3.7 nm, and the average center-to-center distance between adjacent clusters is 5.0 nm. This yields an average gap between clusters of 1.3 nm, which is less than expected if the clusters are each surrounded by a monolayer film of dodecanethiol. Laibinis *et al.* (*11*) determined the thickness of a self-assembled monolayer of dodecanethiol on Au(111) to be 1.2 nm. Because the gap between clusters in Fig. 4A is substantially less than $2 \times 1.2 = 2.4$ nm, alkyl thiols attached to adjacent clusters likely interpenetrate in the region between the clusters.

Unlinked arrays are not very stable. Although they can be imaged with TEM, they are destroyed by SEM imaging or by immersing the substrate in various organic solvents. However, it is possible to covalently link the clusters to each other using double-ended molecular interconnects without destroying the planar array. In addition to physically bonding the clusters to each other, the molecular interconnects also serve as "molecular wires" and provide controlled electronic coupling between adjacent particles.

We have used a number of aryl dithiol and di-isonitrile molecules to form stable LCNs using gold clusters. Aryl dithiols and di-isonitriles completely displace alkyl thiols from a Au(111) surface and form SAMs in which only one end of the molecule is attached to the gold substrate (*12*). These molecules also displace dodecanethiol from the gold clusters in an unlinked array and interconnect neighboring clusters to produce a covalently linked network. Figure 3B shows a schematic representation of the displacement process, and Fig. 4B is a TEM micrograph of an array of 3.7-nm-diameter gold clusters fabricated in the same way as the array in Fig. 4A and then immersed for 12 hours in a millimolar solution of the 2.0-nm-long aryl dithiol (20ADT).
in acetonitrile followed by a 20-min rinse in

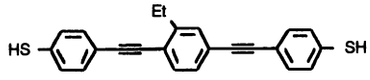

acetonitrile. The average center-to-center distance between adjacent clusters in Fig. 4B is 5.4 nm, which yields an average gap between clusters of 1.7 nm. This increase in the average gap from 1.3 to 1.7 nm indicates that the clusters in Fig. 4B are indeed linked by 20ADT.

The electrical conductance through gold clusters interconnected by aryl dithiol and aryl di-isonitrile molecules has been measured in two ways. In the first experiment, a scanning tunneling microscope (STM) was used to measure the current-voltage characteristics of a bare gold cluster deposited on a dithiol SAM grown on a flat Au(111) surface (*13*). The data obtained are in good agreement with semiclassical predictions for correlated SET. Clusters with diameters <2 nm exhibited "Coulomb staircase" behavior at room temperature. These nanostructures did not exhibit the random offset problems experienced by other SET structures (*14*).

In the second experiment, a linked network of 3.7-nm-diameter clusters was formed in the 450-nm gap between two thin (30 to 40 nm) gold contacts fabricated

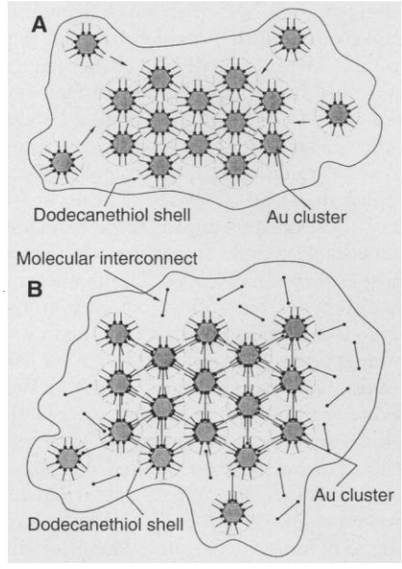

Fig. 3. Self-assembly of a LCN. (**A**) A drop of organic solvent containing dodecanethiol-encapsulated gold clusters is cast on a smooth substrate. On evaporation of the solvent the long-range dispersion forces between clusters cause them to coalesce into a close-packed monolayer. A TEM micrograph of such an unlinked array is shown in Fig. 4A. (**B**) The substrate with its unlinked cluster array is immersed in an acetonitrile solution containing aryl dithiol or di-isonitrile molecules. The molecular interconnects displace the dodecanethiol molecules from the clusters and form rigid molecular linkages between adjacent clusters. A TEM micrograph of such a linked network is shown in Fig. 4B.

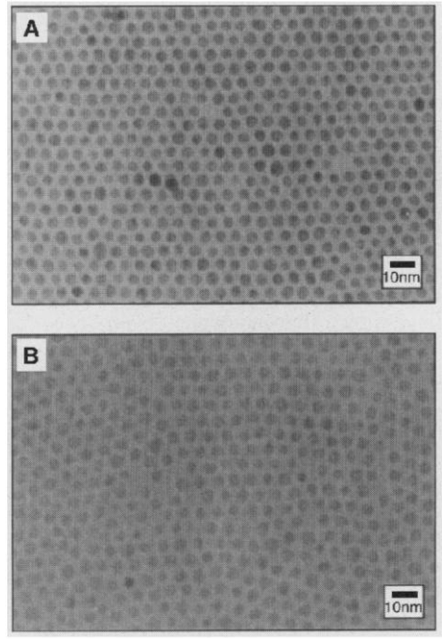

Fig. 4. Bright-field TEM micrographs of monolayer films of 3.7-nm gold clusters supported on a thin flake of MoS_2. (**A**) Unlinked array encapsulated by dodecanethiol. (**B**) Cluster network linked by 20 ADT.

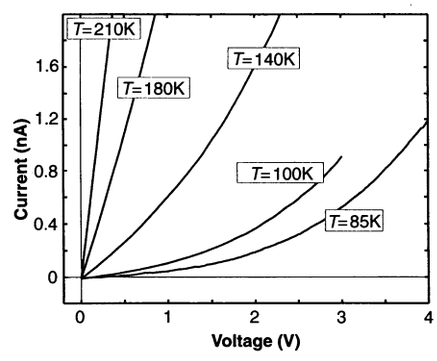

Fig. 5. Measured current-voltage characteristics of a linked cluster network.

on an electron-transparent, free-standing SiO_2 film supported on a GaAs wafer (*15*). A 2.2-nm-long aryl di-isonitrile

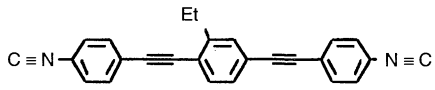

was used to link the clusters. The measured room-temperature conductance of the unlinked array was 133 nS and of the linked network was 78 nS. After a TEM image of the LCN was obtained, the backside of the substrate was metallized and the current-voltage relationship of the LCN was measured as a function of temperature T (Fig. 5).

The low-bias conductance (Fig. 5) exhibits Coulomb charging behavior and followed the relation

$$G_0 = G_\infty e^{-E_A/k_B T} \quad (1)$$

where G_∞ is the conductance as $T \rightarrow \infty$, E_A is an activation energy, and k_B is Boltzmann's constant. The best fit parameters to these data are $G_\infty = 1.12 \times 10^{-6}$S and $E_A = 97$ meV. The capacitance of a cluster embedded in this LCN (cluster diameter of 3.7 nm, and a gap of 1.9 nm, as estimated by TEM) was calculated with the FASTCAP program (*16*) and used to estimate the Coulomb charging energy, which should correspond to E_A for the array. This calculation yields a value of 200 meV/ε_r for E_A (ε_r, the relative dielectric constant of the organic molecules, is estimated to be 1.5 to 2). The agreement with the experimental activation energy, $E_A = 97$ meV, is quite good. The dot-to-dot resistance of this LCN is $R_D \approx (G_\infty)^{-1} = 0.9$ megohm. We estimate the maximum number of molecules linking adjacent clusters to be 32, which would yield an estimated resistance of 29 megohms per molecule. The resistance of a single 22ADI molecule is predicted to be 43 megohms from a semiempirical treatment of a molecule bridging the gap between two gold surfaces by using an extended Hückel method (*17*). The close agreement between these two estimates of molecular resistance indicates that the assumption that the clusters are linked by 22ADI is reasonable.

A general synthesis strategy for fabrication of a 2D network of metal clusters linked by organic molecules has been outlined. The power of this strategy resides in its inherent flexibility. By altering the size or composition of the clusters, the length and chemical structure of the organic molecules used as molecular interconnects, and the characteristics of the substrate, a wide range of electronic behavior can be achieved. Coulomb charging behavior has been observed in such a linked cluster network.

REFERENCES AND NOTES

1. J. R. Tucker, *J. Appl. Phys.* **71**, 4399 (1992); D. Averin and K. K. Likharev, in *Single-Charge Tunneling*, H. Grabert and M. H. Devoret, Eds. (Plenum, New York, 1992); A. N. Korotkov, R. H. Chen, K. Likharev, *J. Appl. Phys.* **78**, 2520 (1995); S. Bandyopadhyay, V. P. Roychowdhury, X. Wang, *Phys. Low-Dimensional Struct.* **8/9**, 29 (1995).
2. G. Schmid *et al.*, *Chem. Ber.* **114**, 3634 (1981).
3. G. Schön and U. Simon, *Colloid Polym. Sci.* **273**, 101 (1995); *ibid.*, p. 202.
4. R. G. Freeman *et al.*, *Science* **267**, 1629 (1995); S. Rubin, G. Bar, T. N. Yaylor, R. W. Cutts, T. A. Zawodzinski, *J. Vac. Sci. Technol. A* **14**, 1870 (1996).
5. M. Brust, M. Walker, D. Bethell, D. J. Schiffrin, R. Whyman, *J. Chem. Soc. Chem. Commun.* **1994**, 801 (1994); D. V. Leff, P. C. Ohara, J. R. Heath, W. M. Gelbart, *J. Phys. Chem.* **99**, 7036 (1995).
6. R. L. Whetten *et al.*, *Adv. Mater.* **8**, 428 (1996).
7. R. S. Bowles, J. J. Kolstad, J. M. Calo, R. P. Andres, *Surf. Sci.* **106**, 117 (1981); S. B. Park, thesis, Purdue University (1988).
8. A. N. Patil, D. Y. Paithankar, N. Otsuka, R. P. Andres, *Z. Phys. D* **26**, 135 (1993).
9. L. C. Chao and R. P. Andres, *J. Colloid Interface Sci.* **165**, 290 (1994).
10. G. E. Poirier and E. D. Pylant, *Science* **272**, 1145 (1996).
11. P. E. Laibinis, R. G. Nuzzo, G. M. Whitesides, *J. Phys. Chem.* **96**, 5097 (1992).
12. J. I. Henderson, G. M. Ferrence, S. Feng, T. Bein, C. P. Kubiak, *Inorg. Chim. Acta* **242**, 115 (1996).
13. M. Dorogi, J. Gomez, R. Osifchin, R. P. Andres, R. Reifenberger, *Phys. Rev. B* **52**, 9071 (1995); R. P. Andres *et al.*, *Science* **272**, 1323 (1996).
14. J. G. A. Dubois, E. N. G. Verheijen, J. W. Gerritsen, H. van Kempen, *Phys. Rev. B* **48**, 11260 (1993).
15. D. B. Janes *et al.*, *Superlattices Microstruct.* **18**, 275 (1995); V. R. Kolagunta *et al.*, *Proc. Electrochem. Soc.* **95-17** (Quantum Confinement), 56 (1996). An early version of this substrate was fabricated by H. Craighead at the Cornell National Nanofabrication Facility.
16. K. Nabors and J. White, *IEEE Trans. Comput. Aided Des. Integrated Circ. Syst.* **10**, 1447 (1991).
17. M. P. Samanta, W. Tian, S. Datta, J. I. Henderson, C. P. Kubiak, *Phys. Rev. B* **53**, R7626 (1996).

18. Funded in part by the Army Research Office under grant DAAL03-G-0144 and the National Science Foundation under grant NSF ECS-9117691. We thank H. Craighead, S. Datta, R. Reifenberger, and M. Samanta for helpful discussions.

26 December 1995; accepted 24 July 1996

A Revised Chronology for Mississippi River Subdeltas

Torbjörn E. Törnqvist,* Tristram R. Kidder, Whitney J. Autin, Klaas van der Borg, Arie F. M. de Jong, Cornelis J. W. Klerks, Els M. A. Snijders, Joep E. A. Storms, Remke L. van Dam, Michael C. Wiemann†

Radiocarbon measurements by accelerator mass spectrometry relating to three of the four late Holocene Mississippi River subdeltas yielded consistent results and were found to differ by up to 2000 carbon-14 years from previously inferred ages. These geological data are in agreement with archaeological carbon-14 data and stratigraphic ages based on ceramic seriation and were used to develop a revised chronologic framework, which has implications for prehistoric human settlement patterns, coastal evolution and wetland loss, and sequence-stratigraphic interpretations.

The geochronology of the Mississippi delta is relevant to investigations of fluvial development in relation to deltaic evolution (*1*, *2*), coastal evolution (*3*), archaeological research (*4*, *5*), coastal wetland loss (*6*), and sequence-stratigraphic interpretations (*7*). For example, the age of subdeltas (*8*) is an important input parameter for simulation models of wetland loss, a severe environmental problem in this region. The chronology of Mississippi River subdeltas is a well-known textbook example of clastic sedimentology (*9*), and it can contribute to computer simulations of alluvial architecture (*10*) where avulsion (channel diversion) is a crucial component. Early stratigraphic studies of Holocene sediments in this region (Fig. 1) revealed a relative chronology that is still largely valid (*11*). The first ^{14}C ages were published in the early 1950s (*12*), and subsequent investigations (*13*, *14*) contributed to the development of a numerical-age chronology for Mississippi River subdeltas, which was later revised toward older ages by Frazier (*15*). His chronology has since been used for most Mississippi delta studies (*1*–*7*). However, some concerns can be raised about Frazier's sampling strategy. Many of his samples cover

T. E. Törnqvist, C. J. W. Klerks, E. M. A. Snijders, J. E. A. Storms, R. L. van Dam, The Netherlands Centre for Geoecological Research (ICG), Department of Physical Geography, Utrecht University, Post Office Box 80115, NL-3508 TC Utrecht, Netherlands.
T. R. Kidder, Department of Anthropology, Tulane University, New Orleans, LA 70118, USA.
W. J. Autin, Institute for Environmental Studies, Louisiana State University, Baton Rouge, LA 70803, USA.
K. van der Borg and A. F. M. de Jong, Robert J. van de Graaff Laboratory, Utrecht University, Post Office Box 80000, NL-3508 TA Utrecht, Netherlands.
M. C. Wiemann, Department of Plant Biology, Louisiana State University, Baton Rouge, LA 70803, USA.

*To whom correspondence should be addressed. E-mail: t.tornquist@frw.ruu.nl
†Present address: Florida Museum of Natural History, University of Florida, Gainesville, FL 32611, USA.